Neuron, Vol. 35, 759–771, August 15, 2002, Copyright ©2002 by Cell Press

Suppression without Inhibition in Visual Cortex

Tobe C.B. Freeman,[2] Séverine Durand,[2] Daniel C. Kiper, and Matteo Carandini[1]
Institute of Neuroinformatics
University of Zurich and
Federal Institute of Technology
Winterthurerstrasse 190
CH-8057, Zurich
Switzerland

Summary

Neurons in primary visual cortex (V1) are thought to receive inhibition from other V1 neurons selective for a variety of orientations. Evidence for this inhibition is commonly found in cross-orientation suppression: responses of a V1 neuron to optimally oriented bars are suppressed by superimposed mask bars of different orientation. We show, however, that suppression is unlikely to result from intracortical inhibition. First, suppression can be obtained with masks drifting too rapidly to elicit much of a response in cortex. Second, suppression is immune to hyperpolarization (through visual adaptation) of cortical neurons responding to the mask. Signals mediating suppression might originate in thalamus, rather than in cortex. Thalamic neurons exhibit some suppression; additional suppression might arise from depression at thalamocortical synapses. The mechanisms of suppression are subcortical and possibly include the very first synapse into cortex.

Introduction

From the initial studies in the 1970s (Benevento et al., 1972; Blakemore and Tobin, 1972) to recent computational models, a broad consensus has evolved around a notion of "cross-orientation inhibition" (Morrone et al., 1982). According to this notion, a V1 neuron is inhibited by other V1 neurons signaling a wide range of different orientations. Cross-orientation inhibition is generally considered a key mechanism. A widely held view is that cross-orientation inhibition acts to refine orientation selectivity (see reviews in Ferster and Miller, 2000; Sompolinsky and Shapley, 1997; Vidyasagar et al., 1996). Another view–which we have advocated–is that cross-orientation inhibition acts to control responsiveness (Carandini and Heeger, 1994; Carandini et al., 1997; Heeger, 1992; Schwartz and Simoncelli, 2001).

Evidence in favor of cross-orientation inhibition is commonly found in the phenomenon of cross-orientation suppression (Allison et al., 2001; Bauman and Bonds, 1991; Bonds, 1989; Carandini et al., 1997; DeAngelis et al., 1992; Morrone et al., 1982; Sengpiel et al., 1998; Sengpiel and Blakemore, 1994). Suppression can be observed by superimposing two grating stimuli: one (the test) with bars at the preferred orientation, and the other (the mask) with bars at a different orientation (Figure 1A). A typical V1 neuron (Figure 1C) responds strongly to the test (first row) and gives little response to the mask (first column). When test and mask are superimposed, however, the mask strongly suppresses the responses to the test. This effect is most evident at high-mask contrasts (bottom rows).

Cross-orientation suppression is thought to be an entirely cortical phenomenon, one that is absent in the lateral geniculate nucleus (LGN). A reason for this view (which we will show to be only partially correct) is that when the same experiment is repeated in an LGN neuron (Figure 1B), the mask does not appear to reduce the responses to the test. Because LGN neurons are not selective for stimulus orientation, the responses to test and mask presented alone are roughly equal (first row and first column). Increasing the contrast of either test or mask further increases the response.

There has been little doubt that suppression is due to inhibition from cortical neurons that respond to the mask. These neurons would (1) have largely overlapping receptive fields because suppression is elicited from a small central region within the receptive field of the V1 neuron (DeAngelis et al., 1992); (2) be selective for a variety of orientations, spatial frequencies, and temporal frequencies because suppression is not selective or broadly selective for these attributes (Allison et al., 2001; Bauman and Bonds, 1991; Bonds, 1989; DeAngelis et al., 1992; Morrone et al., 1982); (3) be largely monocular because (although binocular effects have been observed, Sengpiel et al., 1998) suppression is strongest when test and mask are delivered to the same eye (DeAngelis et al., 1992; Walker et al., 1998). With the possible exception of the last (most cells in cat V1 are binocular; Hubel and Wiesel, 1962), none of the above requirements seems to contradict the view that suppression is caused by intracortical inhibition.

But is this widely held view correct? The sole direct evidence linking suppression to intracortical inhibition is an experiment in which GABA inhibition was blocked in a whole region of cortex (Morrone et al., 1987). Pharmacological experiments of this kind, however, can be difficult to interpret: GABA blockers alter the normal function of a network, with effects that range from a loss of selectivity (Sillito, 1975) to epileptogenesis (Chagnac-Amitai and Connors, 1989). Indeed, early conclusions drawn from similar experiments (Sillito, 1975) have later been challenged (Nelson et al., 1994).

In fact, the evidence for inhibition between neurons selective for different orientations is mixed. Studies involving inactivation of cortical sites suggest that this inhibition is present (Crook et al., 1998; Eysel et al., 1990). More direct measures require intracellular measurements of the range of orientations contributing inhibition and excitation. Some of these measurements have indicated that inhibition is less selective than excitation (Borg-Graham et al., 1998; Martinez et al., 2002), but others have reported that excitation and inhibition

[1]Correspondence: matteo@ini.phys.ethz.ch
[2]These authors contributed equally to this work.

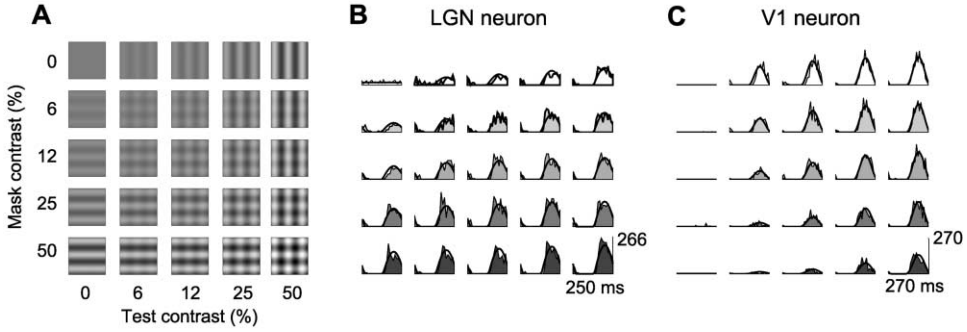

Figure 1. Cross-Orientation Suppression

(A) Stimuli were test gratings drifting in a cell's preferred orientation (first row), mask gratings drifting in an orthogonal direction (first column), and plaids obtained by summing the two (remaining panels). When test and mask have zero contrast, the screen is uniform gray (top left).
(B) Responses of a LGN neuron (neuron 18.3.1, experiment 24.7). Insets indicate firing rate in spikes/s (averaged over 10 ms bins) as a function of time for one stimulus period. Smooth curves indicate fits by the gain control model.
(C) Similar measurements performed with a V1 neuron (neuron 5.3.8, experiment 7.7).

are equally selective (Anderson et al., 2000; Carandini and Ferster, 2000; Douglas et al., 1988).

To avoid the limitations inherent to pharmacological manipulations, we have tested the role of cortical feedback in the generation of suppression with means that are purely visual. We measured suppression caused by visual stimuli that elicit weak or negligible responses in cortex. On the intracortical inhibition hypothesis, these stimuli should cause weaker suppression than stimuli that elicit strong cortical responses.

Results

Suppression constitutes an arithmetical division (Bonds, 1989; Carandini et al., 1997; Heeger, 1992). When the test is presented alone, the mean responses increase sigmoidally with test contrast (Figure 2A, open circles). Increases in mask contrast shift the sigmoid to the right. Because the scale in the abscissa is logarithmic, it is as if the mask had divided the test contrast seen by the cell. This divisive effect is thought to be a key property of cortical visual processing (Heeger, 1992), one that maximizes the independence of cortical neurons as they respond to natural images (Schwartz and Simoncelli, 2001).

We measure suppression by fitting a descriptive model of the responses as a function of test and mask contrast (c_{test} and c_{mask}). This model does not assume a particular mechanism for suppression and is an extension of models found in earlier work on contrast gain control (Albrecht and Geisler, 1991; Carandini et al., 1997; Heeger, 1992). For a typical cortical neuron, the model response R can be approximated by a simple expression:

$$R \approx R_{\max} \frac{c_{test}^{\,n}}{c_{50}^{n} + c_{test}^{n} + (\mathrm{k}c_{mask})^{n}}$$

The behavior of this simplified model is illustrated in Figure 2C. In the absence of a mask ($c_{mask} = 0$), the response is sigmoidal, with R_{max} representing the maximal response and c_{50} representing the half-maximal contrast, where the response is half of R_{max}. Saturation is due to a divisive signal contributed by the test itself.

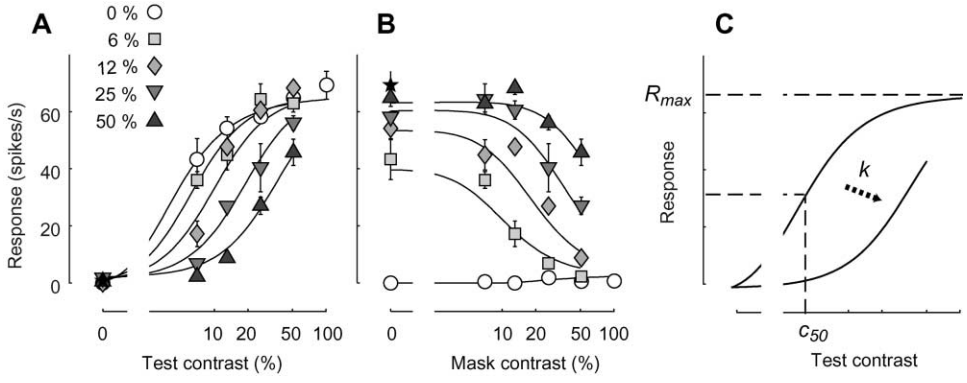

Figure 2. The Divisive Effects of Suppression

(A and B) Mean firing rate of the V1 neuron in Figure 1C as a function of test contrast (A) and mask contrast (B). Curves indicate fits by the gain control model.
(C) Simplified model of suppression. Parameters R_{max}, c_{50}, and k are the maximal response, the half-maximal contrast, and the suppression index.

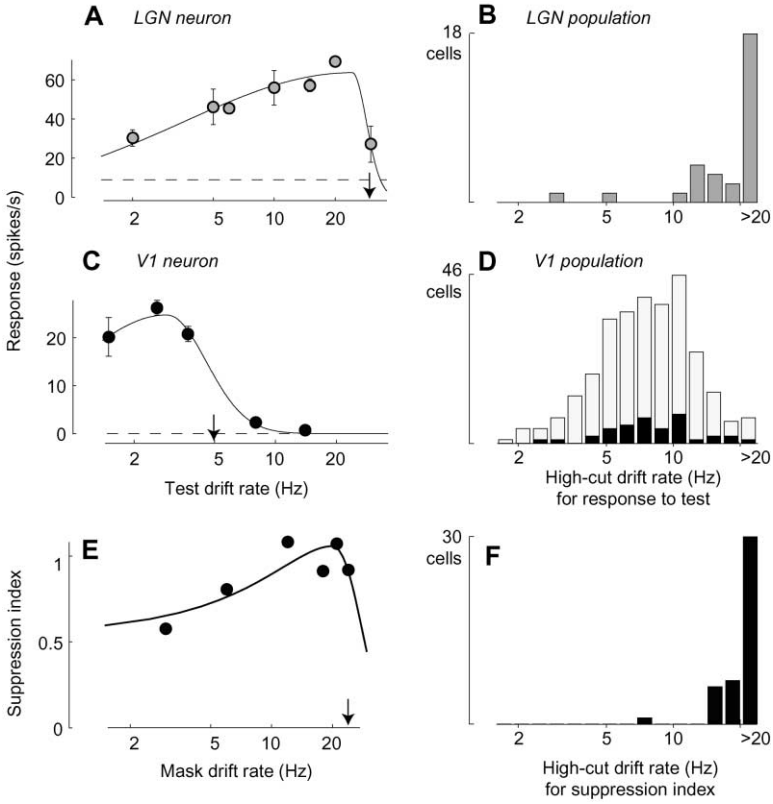

Figure 3. Dependence on Drift Rate of Responses and Suppression

(A) Responses of a LGN neuron as a function of grating drift rate (neuron 8.1.2, experiment 5.2). The arrow indicates the high-cut drift rate, resulting in 50% of maximal response (for this neuron, 29 Hz).

(B) High-cut drift rates for a population of LGN cells (n = 30). Values above 20 Hz are binned in last bar.

(C) Responses of a typical V1 neuron (neuron 11.3.8, experiment 15.5).

(D) High-cut drift rates for a population of V1 cells. Black: some of the 44 V1 cells where we measured suppression. Mean cutoff drift rate is 8.0 ± 1.0 Hz, median 7.9 Hz (n = 38). White: an additional sample of 256 neurons recorded in area 17 or at the 17/18 border.

(E) Suppression index *k* as a function of mask drift rate for the cell in Figure 4. Arrow indicates a conservative estimate of the high-cut rate, at which *k* drops to half the maximum. The true value was >24 Hz, the fastest mask in this experiment.

(F) Distribution of high-cut drift rate for the suppression index.

Suppression is present because the mask also contributes to the denominator. When $c_{mask} > 0$, the sigmoid is shifted to the right to a degree determined by the suppression index *k*. This index measures the ability of the mask to suppress the response (relative to that of the test) and is zero if the mask has no suppressive effect. The model captures the effects of test and mask contrast quite successfully (Figure 1C and Figures 2A–2B).

Suppression with Very Fast Gratings

To probe the sources of suppression, we tested the effects of very fast mask stimuli. Previous measurements have indicated that suppression can be obtained from gratings that drift rather rapidly (Allison et al., 2001; Bonds, 1989; Morrone et al., 1982). We asked whether suppression is evoked by gratings that drift so rapidly that they barely evoke responses in cortex.

Although LGN neurons commonly respond strongly to gratings drifting at rates in excess of 20 Hz (Figures 3A and 3B) (Saul and Humphrey, 1990), gratings drifting so rapidly do not elicit much of a response in V1. Neurons in cat V1 prefer gratings drifting at rates below 10 Hz and barely respond to rates above 15 Hz (DeAngelis et al., 1993; Ikeda and Wright, 1975; Movshon et al., 1978; Saul and Humphrey, 1992). For example, for the V1 neuron in Figure 3C, the high-cut drift rate is only 5.1 Hz, and the response is zero beyond 10–15 Hz. We measured cutoff drift rate in a large sample of V1 neurons (Figure 3D) and found it to average 7.5 ± 1.0 Hz (median 7.7 Hz, n = 294), a value consistent with previous reports (Ikeda and Wright, 1975).

In a small sample of V1 neurons, we performed an additional control measurement to ensure that gratings drifting rapidly are ineffective for V1 cells also when presented in a plaid. We compared cutoff drift rate measured with gratings alone (as in Figures 3C and 3D) and in the presence of an orthogonal grating. In the presence of the orthogonal grating, cutoff drift rate increased only slightly by a factor of 21% ± 11% (SEM, n = 9). This slight increase is consistent with previous results involving sums of gratings (Reid et al., 1992). The small size of the effect confirms that gratings drifting rapidly are ineffective visual stimuli for V1 cells whether they are presented alone or as part of a plaid.

Though unable to drive V1, fast drifting gratings cause powerful suppression. An example of this behavior is illustrated in Figure 4. When test and mask are both drifting slowly (3 Hz, Figure 4A), the mask elevates the half-maximal contrast from 23.0% to 45.2%. The corresponding suppression index is *k* = 0.6. Increasing mask drift rate does not reduce suppression, with an index of 0.8 for 6 Hz masks (Figure 4B), of 1.1 for 12 Hz masks (Figure 4C), and of 0.9 for 24 Hz masks (Figure 4D). A plot of the suppression index *k* as a function of mask drift rate summarizes these effects and indicates the high-cut drift rate that results in 50% of maximal suppression (Figure 3E). Suppression with fast stimuli was so strong that the high-cut drift rate for *k* lay somewhere beyond 24 Hz, the fastest mask tested. Suppression was obtained with very fast masks in most cells in our sample: the high-cut drift rate for the suppression index was high, 19.4 ± 3.1 Hz (SD, n = 44), with a median value of 19.6 Hz (Figure 3F). These numbers underestimate the true values: just like for the cell in Figure 4, in 26/44

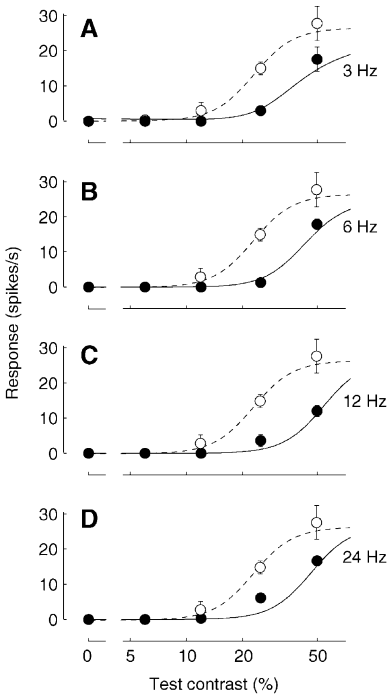

Figure 4. Suppression with Very Fast Mask Stimuli

Responses of a V1 neuron to an optimal test grating, drifting at 3 Hz, alone (open circles) and in the presence of an orthogonal mask (closed circles) drifting at 3 Hz (A), 6 Hz (B), 12 Hz (C), and 24 Hz (D). Neuron 11.3.8, experiment 15.11.

cells, the high-cut drift rate was beyond the highest drift rate used in the experiment (20–24 Hz). Rather than extrapolating it, we conservatively set it to this value.

These observations are not consistent with the view that the signals responsible for suppression originate in cortex. Visual responses in cat cortex must pass through areas 17 or 18 (Payne and Peters, 2002). Though neurons in area 18 respond to slightly faster stimuli than those in area 17 (Movshon et al., 1978), neurons in either area give less than 10% of their maximal response to stimuli drifting faster than 15–20 Hz (Ikeda and Wright, 1975; Saul and Humphrey, 1992). For most V1 neurons, however, masks drifting as rapidly as 20 Hz caused more than 50% of maximal suppression. Indeed, the distribution of high-cut drift rates of the suppression index (Figure 3F) is very different from that of V1 responses (Figure 3D). Rather, it resembles that of LGN responses (Figure 3B).

Suppression following Cortical Adaptation

We have argued that the cortex could not contribute suppression signals evoked by a mask drifting rapidly. Still, the cortex could in principle contribute suppression signals when masks drift slowly. Is this the case? To address this question, we measured suppression after reducing selectively and reversibly the activity of those V1 neurons that respond to the mask. To reduce the activity of cortical neurons, we exploited the phenomenon of visual adaptation that follows prolonged stimulation. Visual adaptation leaves LGN neurons largely unaffected (Sanchez-Vives et al., 2000; Shou et al., 1996) while substantially reducing the responses of V1 neurons (Albrecht et al., 1984; Maffei et al., 1973; Ohzawa et al., 1985). This reduction is caused by a tonic hyperpolarization (Carandini and Ferster, 1997; Sanchez-Vives et al., 2000), which only affects those neurons that are activated by the prolonged stimulus (Carandini et al., 1998). If suppression were to be immune to such adaptation, it would be unlikely to originate from intracortical signals.

Adaptation to a grating strongly reduces the responses of neurons that are selective for the grating and very slightly reduces the responses of neurons selective for orthogonal gratings. Adaptation to an optimal test stimulus (Figures 5A and 5B) shifts the contrast response curves down and to the right (Albrecht et al., 1984; Ohzawa et al., 1985). For the V1 cell in Figure 5A, it reduced the maximum response R_{max} by a factor of 1.8 (from 64.5 $\pm$ 0.7 to 35.3 $\pm$ 0.9 spikes/s, SD, bootstrap estimates) and greatly increased the half-maximal contrast c_{50} by a factor of 5.0 (from 4.6% $\pm$ 0.3% to 23% $\pm$ 1.9%). Indeed, at a test contrast of 6%, the robust response measured when adapting to a gray screen had vanished. Similar results were obtained for the whole population (Figure 5B): adaptation to an optimal test dramatically reduced the maximal response (by a factor of 1.6 $\pm$ 1.1, SEM, n = 28) and increased the half-maximal test contrast (by a factor of 2.2 $\pm$ 1.1). Adaptation did not spare any cell. In those cells (5/28) where the increase in half-maximal test contrast was $<$1.5, maximal response was reduced by $>$1.25. Adaptation to an orthogonal mask (Figure 5C) was overall much weaker and had effects that varied from cell to cell (Carandini et al., 1998). It reduced maximal response by an insignificant amount (a factor of 1.1 $\pm$ 1.1, n = 30) and increased half-maximal test contrast by a small degree (a factor of 1.5 $\pm$ 1.1) compared to adaptation to an optimal stimulus.

Unlike the responses of cortical neurons, we found suppression to be largely immune to adaptation. For our example cell, suppression remained strong even following adaptation to the mask (Figure 6A). As mask contrast increases from 0% to 50% (open circles to closed triangles in Figure 6A), half-maximal test contrast increases nearly 4-fold, just as it did in the control condition (Figure 2A). In fact, when measuring the suppression index for this cell (Figure 6C, closed circles), one sees no significant change (from 0.80 $\pm$ 0.05 following adaptation to a gray screen to 0.86 $\pm$ 0.06 following adaptation to the mask). Similar results were obtained for the rest of our population (open circle): following adaptation to the mask, the suppression index is mildly increased in some cells (16/30) and mildly decreased in others (13/30), with no consistent or strong effects in either direction (mean change: 17% $\pm$ 64%, median = 1%).

This immunity to adaptation is hard to reconcile with the hypothesis that suppression originates from intracortical inhibition from neurons responding to the mask orientation. One would need an explicit model of adaptation and cross-orientation inhibition to predict how much adaptation should have reduced suppression. Here, however, we just tested the simple qualitative prediction that such a reduction would occur and found it to be wrong.

Finally, we considered the possibility that suppression

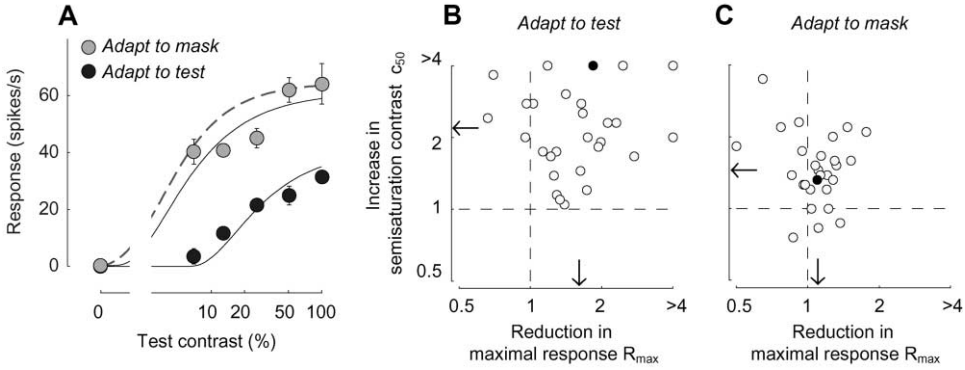

Figure 5. Adaptation to an Optimal Stimulus, But Not to an Orthogonal Stimulus, Dramatically Reduces the Responses of V1 Neurons

(A) Responses of the V1 neuron of Figure 2 to the test following adaptation to the mask (gray) or to the test (black). Neuron 5.3.8 expts. 7.8-10. Continuous curves: fits of the model. Dashed curve is reported from Figure 2A to facilitate comparison with the responses following adaptation to the gray screen.

(B) Summary of effects of adaptation to an optimal stimulus. Effects of adaptation to the test on the maximal response R_{max} (abscissa) and on the half-maximal contrast c_{50} (ordinate) for the example cell (closed circles) and for the remaining cells (open circles).

(C) Same, for adaptation to the mask.

might be caused by intracortical inhibition from some hypothetical visual area that does not respond well to gratings but gives strong responses to plaids obtained by superimposing test and mask. Neurons in such an area would be largely immune to adaptation to the mask and, thus, would continue to provide strong suppression following this adaptation condition. Their responses, however, would be reduced by adaptation to the plaid. Adaptation to the plaid would then reduce the strength of cross-orientation suppression. We tested this prediction by looking at the effects on suppression of adaptation to plaids, and found it incorrect. Overall, rather than being reduced, the suppression index following adaptation to the plaid was mildly increased (data not shown). This mild increase is consistent with previous observations (Carandini et al., 1998). As with adaptation to single gratings, suppression is immune to adaptation to plaids.

Suppression in LGN

The properties of suppression in V1 neurons that we have demonstrated—effectiveness of high drift rates and immunity to adaptation—are inconsistent with signals originating in visual cortex. These properties, instead, would be easily explained if the relevant signals originated in LGN.

In particular, one might ask whether some degree of suppression is already present in the responses of LGN neurons and then simply passed on to V1. We recorded from LGN neurons and found that this is the case. LGN neurons can exhibit some degree of suppression.

The response of LGN neurons to gratings saturates with contrast, and this saturation is a form of suppression. Consider, for example, the LGN neuron of Figure 1B. Not being selective for orientation, the neuron responds both to the test (top row) and to the mask (left column). As contrast increases, though, the response exhibits a mild degree of saturation (e.g., Ohzawa et al., 1985). For example, as contrast doubles from 25% to 50%, response grows by less than a factor of two. This saturation entails a form of suppression. When test and mask are summed together (middle panels), increments in test contrast or in mask contrast have even less effect

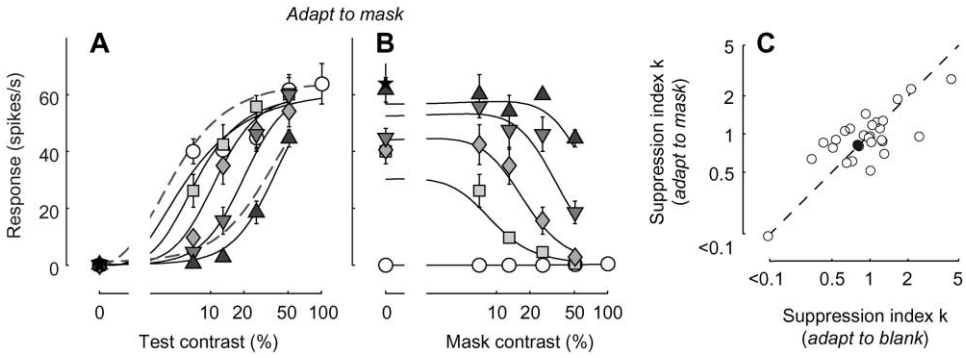

Figure 6. Effects on Suppression of Adaptation to the Mask

(A and B) Effects of adaptation on the responses of the example V1 neuron (neuron 5.3.8, experiments. 7.8–10). Dashed curves are reported from Figure 2A to facilitate comparison with those following adaptation to the gray screen.

(C) Effects of adaptation on the suppression index *k* for the example cell (closed circles) and for the remaining cells (open circles) (n = 28). Values are measured following adaptation to a gray screen (abscissa) and following adaptation to the mask (ordinate). Ranges are matched, so if *k* is unaffected by adaptation, the corresponding symbol lies on the diagonal.

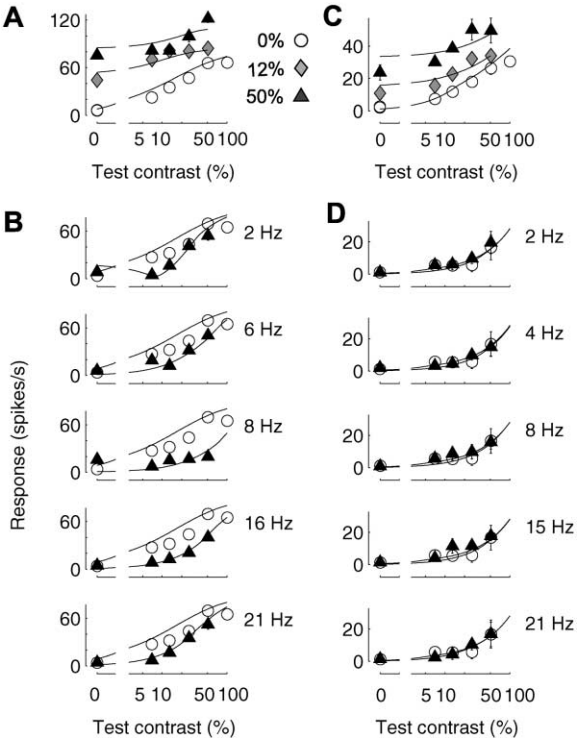

Figure 7. Suppression in LGN

(A) Response as a function of test contrast for three mask contrasts (0%, 12%, and 50%). Test and mask drifted at 4 Hz, and the ordinate reports the 4 Hz component of the responses. These are the same data as in Figure 1B (neuron 18.3.1, experiment 24.7). Curves indicate fits by a simple model (Experimental Procedures).

(B) Responses of the same cell to the 4 Hz test in the presence of masks of different drift rate (experiment 24.10).

(C and D) Similar data for another LGN neuron (neuron 17.1.5, experiments 11.9–10). Here the test drifted at 5 Hz, and the ordinates report the 5 Hz component of the response.

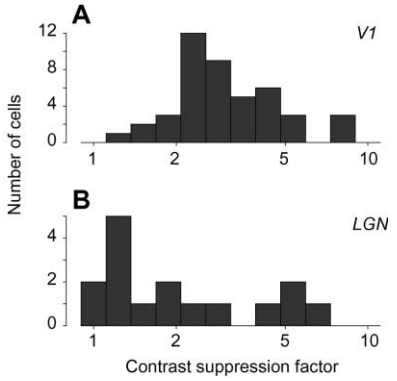

Figure 8. Strength of Suppression in LGN and V1

Contrast suppression factor is ratio of half-maximal test contrast in the presence and absence of a 50% contrast mask.

(A) V1 neurons (median: 2.95, n = 44).

(B) LGN neurons (median: 1.61, n = 16).

on the responses. The mask has strongly suppressed the incremental response related to the test. These effects are well captured by a descriptive model (fitted curves) that is similar to the one used for V1 neurons (see Experimenal Procedures).

The effects of saturation can be observed more clearly when one plots responses as a function of test contrast for different mask contrasts (Figure 7A). In the absence of a mask (open circles), responses grow with contrast but tend to saturate at high contrasts, particularly between 50% and 100%. As mask contrast is increased, the incremental effect of test contrast is further suppressed (closed diamonds, closed triangles). This suppression appears less dramatic than that observed in V1 (Figure 2A), where an increase of mask contrast leads to a response reduction. However, the two effects are analogous, with suppression being less evident in LGN because neurons there respond to both test and mask.

Suppression in LGN neurons becomes clearer once the drift rates of mask and test are made to differ (Figure 7B). The response to the test can then be isolated from the response to the mask by considering the modulation in response at the test frequency (Bonds, 1989). For this LGN neuron, this component is clearly suppressed by the mask (compare open circles and closed triangles) whether the mask is drifting slowly (top) or rapidly (bottom). Indeed, the results of this experiment bear some resemblance to the results of the similar experiment performed on a V1 neuron (Figure 4).

Not all LGN neurons exhibit suppression. For the neuron in Figure 7D, for example, the mask leaves the response to the test unaffected. Consistent with the view that saturation and suppression are related phenomena, this neuron also showed less response saturation (Figures 7C and 7D) than the one in Figures 7A and 7B. Saturation and suppression might be manifestations of retinal contrast gain control (Shapley and Victor, 1981; 1978) or simply reflect a nonlinearity in the output of individual LGN neurons.

Suppression in LGN is generally weaker than in V1. To make the comparison, we considered a contrast suppression factor by measuring the reduction in an effective test contrast caused by the mask. We defined this factor as the ratio between half-maximal test contrast in the presence and absence of the mask. A factor of two, for example, indicates that the cell required twice as much test contrast to obtain a given response with the mask than without the mask. The contrast suppression factor is obtained directly from the curves fitted to the responses, not from model parameters. The latter would not be comparable, as descriptive models required to fit responses of LGN and V1 neurons are different. In our population of V1 neurons, the contrast suppression factor ranges from 1.33 to 8.69, with a median of 2.95 (Figure 8A). The distribution for LGN neurons is widely spread and is shifted toward lower values, with a median of 1.61 (Figure 8B). Indeed, suppression in most LGN cells was intermediate between the extremes represented by the cells in Figure 7. Some LGN neurons show substantial suppression, with contrast suppression factors as large as 5.96. Most LGN cells, however, show little suppression, with contrast suppression factors as low as 1.10, lower than most V1 neurons.

While suppression in LGN is unlikely to fully explain suppression in V1, it is not easy to gauge from Figure 8 the exact extent of its contribution. Indeed, our analysis

suffers from a number of limitations. First, our sample of LGN neurons is small. Second, rather than lumping neurons together, one would need a notion of which LGN neurons should be compared with which V1 neurons. Third, visual stimuli employed in LGN and V1 were similar, but not identical. Test gratings had drift rate, size, and spatial frequency optimized for the cell being recorded, and these attributes could be different in LGN and V1. Moreover, the contrast suppression factor was computed for the mask yielding maximal suppression, and again the drift rate of this mask could be different in LGN and V1. Although matching neuronal samples and visual stimuli across areas is difficult, future work could certainly improve on our measurements.

Discussion

We have shown that powerful suppression can be obtained with masks drifting too rapidly to elicit much of a response in cortex. Moreover, suppression is immune to visual adaptation of cortical neurons that respond to the mask.

There are reasons to believe that these results can be extended from the cortex of anesthetized cats to that of awake humans. Indeed, our results are in excellent agreement with perceptual suppression effects. Perceptually, the contrast needed to detect a test grating is increased by the presence of an orthogonal mask grating. Just as in our physiological results, this perceptual suppression is largely immune to adaptation to the mask (Foley and Chen, 1997) and is present also with a mask that drifts very rapidly (Boynton and Foley, 1999; Meier and Carandini, 2002).

One possible explanation of our results is that suppression is mediated by inhibition and that the inhibitory interneurons responsible for it (1) are immune to visual adaptation and (2) respond strongly to gratings drifting faster than 20 Hz. This explanation, however, is unlikely because we did not encounter neurons with these properties, and we do not know of any report of their existence. Consider first the case of adaptation. Consistent with previous reports (Albrecht et al., 1984; Sanchez-Vives et al., 2000), all neurons in our sample saw their response reduced following adaptation to an optimal stimulus (Figure 5B). Indeed, the fact that inhibitory interneurons exhibit little spike frequency adaptation (McCormick et al., 1985) does not imply that they exhibit little visual adaptation. Visual adaptation can be obtained in the absence of spikes, so it does not involve mechanisms of spike frequency adaptation (Carandini and Ferster, 1997; Sanchez-Vives et al., 2000). Consider now the case of gratings drifting very rapidly. Consistent with previous reports (DeAngelis et al., 1993; Movshon et al., 1978; Saul and Humphrey, 1992), we find only a handful of neurons responding to gratings drifting at about 20 Hz (Figure 3D), and we know that these neurons do not respond to faster gratings. Yet in many cells (e.g., Figure 3A), suppression gave no sign of abating around 20 Hz, and the values that we report for its cutoff are conservatively underestimated. We conclude that the putative inhibitory interneurons responsible for suppression would have to be invisible to our electrodes. This possibility, however, seems remote. While extracellular recording may introduce a sampling bias (Robinson, 1968), it is not at all blind to spikes from inhibitory interneurons (Cohen and Miles, 2000).

A proposal that suppression might originate in area 18 (Allison et al., 2001) seems similarly unlikely. As we have shown in Figure 3D (which includes data from the 17/18 border) and as others have shown before (Movshon et al., 1978), neurons in area 18 barely respond to such high drift rates. Moreover, connections between areas 18 and 17 are thought to be excitatory (Gilbert and Kelly, 1975), and there is little reason to believe that neurons in area 18 would be immune to adaptation.

A simpler explanation of our results is that the source of suppression lies in feedforward thalamic signals, not in the cortical network. Indeed, neurons in LGN respond to high drift rates (Figure 3A), and there is a strong similarity between the high-frequency cutoffs for the responses of LGN neurons (Figure 3B) and for the strength of suppression (Figure 3F). Moreover, the responses of LGN neurons show little adaptation, if any (Ohzawa et al., 1985; Sanchez-Vives et al., 2000; Shou et al., 1996). Finally, LGN neurons also easily meet the remaining requirements (Bauman and Bonds, 1991; Bonds, 1989; DeAngelis et al., 1992; Morrone et al., 1982; Walker et al., 1998): they are monocular, and they are individually (not only as a group) broadly tuned for stimulus orientation and spatial and temporal frequency. In fact, the possibility that suppressive signals might originate in LGN has been considered before (Nelson, 1991c; Walker et al., 1998), but the lack of a mechanism for this suppression has stymied progress: how could a suppressive signal from LGN reach cortical neurons?

The most prosaic explanation, that some suppression is already present in the responses of LGN neurons (Figure 7), is not likely to be sufficient. Our comparison of LGN and V1 (Figure 8) indicates that suppression in LGN is not strong enough to explain the full extent of V1 suppression. A number of additional observations confirm this view. First, saturation of responses with increasing contrast is stronger in V1 than in LGN. This can be seen in our data (compare Figure 2 and Figure 7) and has been demonstrated for the macaque visual system (Sclar et al., 1990). There is little reason to doubt that the mechanisms of suppression are the same that cause saturation. Suppression can be strong for all mask orientations (Bonds, 1989; DeAngelis et al., 1992; Morrone et al., 1982), including the preferred orientation of the cell. Because doubling the contrast of a test grating is equivalent to adding to the test an identical mask, suppression is equivalent to saturation. Second, suppression in V1 is observed also with masks of low contrast (Figure 2), which might not cause enough saturation and suppression in LGN (Figure 7). Third, if instead of drifting gratings one uses test and mask that are flashed bars, one finds strong suppression in V1 (Nelson, 1991a) and no suppression in LGN (Nelson, 1991b). This form of suppression is not due to intracortical inhibition (Nelson, 1991c) and appears to have a memory of a few hundred milliseconds (Nelson, 1991a), which is not present in the responses of LGN neurons (Nelson, 1991b).

As a result, suppression likely involves additional mechanisms beyond those affecting the responses of LGN neurons. These mechanisms would have to be thalamocortical and operate somewhere between the out-

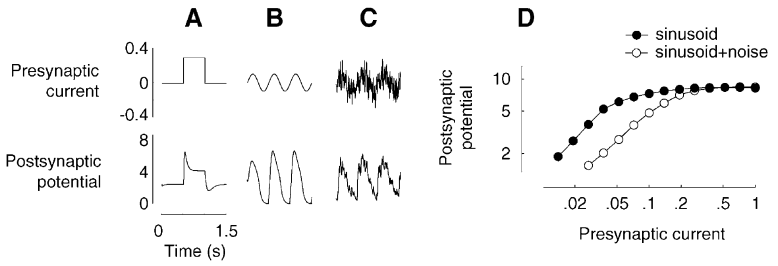

Figure 9. Saturation and Suppression in a Model Depressing Synapse

(A–C) Effects of current injection of various waveforms into the presynaptic neuron. Top, current injected into presynaptic neuron ([A], step; [B], 2 Hz sinusoid; [C], sinusoid plus white noise). Bottom, postsynaptic potential after the current has been filtered by the passive properties of the neuron. To avoid unnecessary free parameters, we have used arbitrary units for currents and potentials.

(D) The 2 Hz component of the postsynaptic potential *V* as a function of presynaptic sinusoidal current amplitude.

put of LGN neurons and that of V1 neurons. Possible sites could be the dendrite of V1 neurons (as in Koch et al., 1983) or the synapse between LGN and V1 through synaptic depression.

Thalamocortical Synaptic Depression

We favor the latter possibility, and suggest that the additional mechanism at work is depression at thalamocortical synapses. Depression at these synapses has been observed in vitro (Stratford et al., 1996) and in vivo (Chung et al., 2002; Ferster and Lindström, 1985; Sanchez-Vives et al., 1998, Soc. Neurosci. Abst.). Depression might contribute to temporal response characteristics of V1 cells such as direction selectivity (Chance et al., 1998) and the sharp transients in response to contrast steps (Müller et al., 2001). Together with other biophysical mechanisms, depression has been suggested to contribute to a variety of behaviors exhibited by V1 neurons (Kayser et al., 2001; Lauritzen et al., 2001). In collaboration with David Heeger and Walter Senn, we have explored the degree to which thalamocortical synaptic depression alone can explain phenomena previously attributed to intracortical inhibition.

The responses of a depressing synapse are transient, and exhibit saturation and divisive suppression (Figures 9B–9D). Consider the response of a model depressing synapse to a presynaptic step of current (Figure 9A). As presynaptic current steps up (top), postsynaptic potential increases rapidly but is cut short by synaptic depression (bottom). The sharp transient is followed by a plateau and then by recovery at the end of the step. These properties of depression might explain the transient responses of V1 cells to flashed stimuli (Müller et al., 1999, 2001; Tolhurst et al., 1980). Consider now the responses to a sinusoidal-injected current (Figure 9B). Depression distorts the postsynaptic current, which is not sinusoidal. Distortion increases with presynaptic firing rate, causing a substantial saturation in response amplitude (Figure 9D, open circles) (Abbott et al., 1997; Kayser et al., 2001; Tsodyks and Markram, 1997). Adding noise to the injected current (Figure 9C) increases synaptic depression. The noise partially suppresses the responses to the sinusoidal current (compare Figures 9B and 9C, bottom rows). This suppression is divisive (Figure 9D, rightward shift of the curves on the logarithmic scale), as if the noise had divided the amplitudes of the test currents by a fixed factor.

To explore the degree to which it can explain visual properties, we included thalamocortical synaptic depression in a simplified model of V1 simple cell (Hubel and Wiesel, 1962). In the model, orientation selectivity is determined by the spatial pattern of LGN inputs, with ON and OFF subregions of the receptive field (Figure 10A) being driven by excitation from ON-center and OFF-center LGN neurons (Alonso et al., 2001; Reid and Alonso, 1995) (Figure 10B). Excitation is complemented by subtractive inhibition arranged in push-pull fashion, whereby excitation by ON-center neurons is matched by inhibition by OFF-center neurons and vice versa (Ferster, 1988; Glezer et al., 1982; Hirsch et al., 1998; Palmer and Davis, 1981; Tolhurst and Dean, 1987, 1990). In reality, inhibition would be provided by cortical interneurons (Palmer and Davis, 1981; Troyer et al., 1998). To judge the contribution of depression alone, we did not include in the model any saturation or suppression in LGN signals.

Synaptic depression would explain cross-orientation suppression (Figure 10). Thanks to the spatial pattern of synapses, the model V1 cell gives strong responses to test (Figure 10C) and no response to the orthogonal mask (Figure 10D). Thanks to synaptic depression, the response to plaid (Figure 10E) is smaller than the response to test alone (Figure 10C). The individual LGN neurons are not selective for orientation so both test and mask cause an equally strong synaptic depression. Depression is even stronger in response to the plaid obtained by summing test and mask because two superimposed stimuli cause more synaptic depression than either stimulus alone (Figure 9). By contrast, without synaptic depression, the responses to the plaid would have been as large as the responses to the test (Figure 10E, dashed curve). Because the effects of synaptic depression are divisive (Figure 9), the model correctly predicts that the effects of suppression are divisive. The main effect of increasing mask contrast is to shift the curves to the right (Figure 10F). In the logarithmic contrast scale, this shift corresponds to division of the effective test contrast. This behavior strongly resembles that shown by real V1 neurons (Figure 2A). These effects would be even stronger if one were to include in the model the observed saturation/suppression of LGN responses.

Thalamocortical synaptic depression would explain the properties of V1 neurons that we have described in the Results section. First, it would explain response saturation with increasing contrast (Figure 10F): depression grows with presynaptic activity, which would grow with contrast. Second, it would explain why suppression

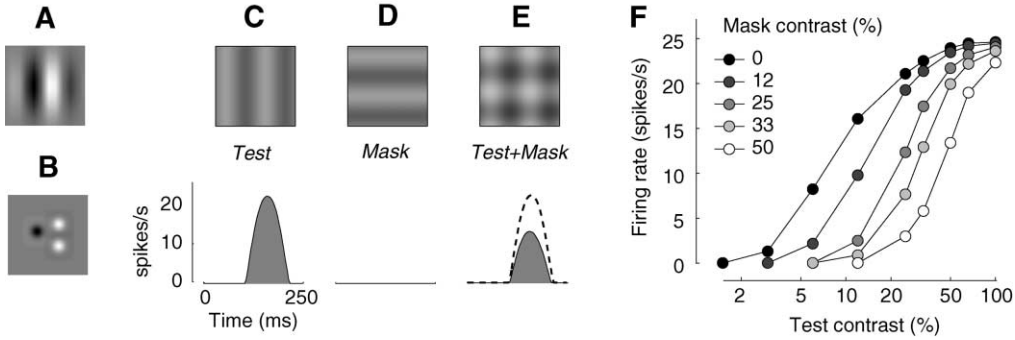

Figure 10. Cross-Orientation Suppression Explained by Thalamocortical Synaptic Depression

(A) Receptive field of the model V1 neuron.

(B) Examples of receptive fields of model LGN neurons, two ON-center and one OFF-center.

(C–E) Responses to gratings and plaids. Top: one frame of the stimulus. Bottom: mean responses of model V1 neuron to a stimulus cycle. Stimuli are a rightward drifting vertical grating (C), a downward drifting horizontal grating (D), and the plaid obtained by summing the two (E). Dashed curve is the response to the plaid in the absence of synaptic depression. Gratings drift at 4 Hz and have 20% contrast.

(F) Suppression in model responses. Different curves correspond to different mask contrasts.

can be obtained with masks drifting too rapidly to drive cortical neurons (Figure 3): LGN neurons would respond to these masks, and their synapses would be further depressed. Third, it would explain why suppression is immune to adaptation (Figure 6): rapid depression recovers with a time constant of tens to hundreds of milliseconds (Abbott et al., 1997; Thomson and Deuchars, 1997; Varela et al., 1997), shorter than the 1–2 s interval between our adapting stimuli and the subsequent probe stimuli.

Thalamocortical synaptic depression would also explain other properties of suppression (M.C., D.J.H., and W.S., unpublished data), including a discrepancy in the literature about whether suppression is selective for orientation. Suppression has been reported to be broadly tuned for mask orientation, often equally strong when mask and test are parallel as when they are orthogonal (Bonds, 1989; DeAngelis et al., 1992; Morrone et al., 1982). Suppression has also been reported to be selective for mask orientation, often completely absent when test and mask are orthogonal (Nelson, 1991a). The depression model ascribes this discrepancy to the type of mask used: the former studies employed drifting grating masks, which at any orientation depress all the synapses in their path; The latter study employed flashed bar masks, which depress only a limited set of synapses.

Among the testable predictions of our model is that the time courses of suppression and depression should be consistent, both for onset and for recovery. In our data, suppression takes place in the very beginning of the responses to test and mask, with a time course faster than we can resolve. Responses of simple cells oscillate with the period of the stimulus (e.g., 250 ms in Figure 1C), so we cannot resolve faster events. Responses of complex cells are irregular and did not reveal prominent transients at stimulus onset. Moreover, we did not collect responses to test following mask withdrawal, so we cannot speculate on the time required to recover from suppression. An appropriate way to measure these time courses is by independently introducing and withdrawing test and mask in rapid random succession. This was recently done by Smith et al. (2001), who reported that cross-orientation suppression is about 20 ms slower than the reduction in response caused by removal of the optimal test stimulus. This value is consistent with synaptic depression: while depression follows a presynaptic spike immediately, a few spikes might be required to reach steady state. Smith et al. also found that recovery from suppression followed a similar 20 ms delay, at the low end of published estimates for the time constant of recovery from synaptic depression (Abbott et al., 1997; Thomson and Deuchars, 1997; Varela et al., 1997).

Surround Suppression

We have argued that cross-orientation suppression in V1 neurons should not be attributed to intracortical inhibition. We have ascribed this phenomenon to gain control mechanisms already present in LGN responses, with the likely help of mechanisms—such as synaptic depression—affecting the transformation of LGN outputs into V1 inputs. This thalamic/synaptic explanation, however, is not meant to explain all the mechanisms that control the gain or responsiveness of V1 neurons.

In particular, it is not meant to apply to surround suppression. Surround suppression is the reduction in responsiveness caused by masks surrounding the center of the classical receptive field (see Fitzpatrick, 2000 for review). Surround suppression is likely to originate from a different mechanism than cross-orientation suppression (Sengpiel et al., 1998) due to cortical signals (Hubel and Wiesel, 1965) possibly involving cortico-thalamic loops (Murphy et al., 1999; Murphy and Sillito, 1987). Unlike cross-orientation suppression, surround suppression is selective for orientation (Blakemore and Tobin, 1972; DeAngelis et al., 1994; Li and Li, 1994) and can be obtained with the test in one eye and the mask in the other eye (DeAngelis et al., 1994). Measurements of membrane conductance (Anderson et al., 2001) and experiments involving inactivation of layer 6 with GABA (Bolz and Gilbert, 1986; but see Grieve and Sillito, 1991) further support the intracortical explanation of surround suppression. Finally, the synaptic depression explanation that we have proposed would not extend to sur-

round suppression. Surround suppression is commonly observed when the masks do not overlap the center of the receptive field (Blakemore and Tobin, 1972; Fitzpatrick, 2000), whereas cross-orientation suppression originates largely from the central region of the receptive field (DeAngelis et al., 1992) where thalamocortical synapses would be expected to be strongest.

Our thalamic/synaptic explanation is also not meant to explain reports of dichoptic cross-orientation suppression (Sengpiel et al., 1998). This form of suppression seems to fall into the category of binocular rivalry (Blake, 2001; Sengpiel et al., 1995) as its effects can take hundreds of milliseconds to reach peak strength (F. Sengpiel, personal communication). Dichoptic suppression must be due to intracortical effects, perhaps to lateral inhibition.

Conclusions

To summarize, the view of cortical function that has evolved since the first demonstrations of suppression might need to be revised. This view posits that suppression arises from lateral inhibition from other cortical neurons and dominates a number of reports from us (Carandini and Heeger, 1994; Carandini et al., 1997) and from our colleagues (Allison et al., 2001; Bauman and Bonds, 1991; Bonds, 1989; DeAngelis et al., 1992; Heeger, 1992; Morrone et al., 1982; Sengpiel et al., 1998, 1995; Sengpiel and Blakemore, 1994; Walker et al., 1998). Our results instead indicate that the source of suppression does not lie in the cortical network. Rather, suppression is likely to originate from feedforward thalamic signals. With the exception of one pharmacological study (Morrone et al., 1987), this explanation is consistent with all that is known about suppression, including a number of observations that would be hard to explain with intracortical inhibition. Suppression in V1 is partially explained by properties of the LGN responses and is likely to be enhanced by mechanisms—such as synaptic depression—affecting the transformation of LGN outputs into V1 inputs. An important element of visual processing lies in the circuit leading to the cortex, possibly including the very first synapse into the cortex.

Experimental Procedures

Our methods for recording from anesthetized cats are standard and have been described elsewhere (e.g., Carandini and Ferster, 2000). Briefly, adult cats were anesthetized with ketamine (20 mg/kg) and acepromazine (0.1 mg/kg) and premedicated with atropine sulfate (0.05 mg/kg). Anesthesia was maintained with a continuous IV infusion of penthotal (1–4 mg/kg/hr). Animals were paralyzed with pancuronium bromide (0.15 mg/kg/hr) and artificially respired. EEG, ECG, and end-tidal CO_2 were continuously monitored. Extracellular signals were recorded with glass-coated tungsten microelectrodes, sampled at 12 kHz, and stored for offline spike discrimination. The veterinary office of Canton Zurich approved all procedures.

Visual stimuli were plaids composed of two drifting sinusoidal gratings, displayed using the Psychophysics Toolbox (Brainard, 1997; Pelli, 1997) and presented monocularly. Gratings had optimal spatial frequency, position, and size. The test grating drifted in the cell's preferred direction and rate (2–5 Hz), while the mask grating drifted in an orthogonal direction. Stimuli lasted 1–4 s and were presented in randomized order. Adaptation stimuli were presented initially for 30 s and then for 3–6 s prior to the presentation of each stimulus (Carandini and Ferster, 1997; Movshon and Lennie, 1979). Adapting stimuli had 50% contrast.

V1 neurons were in area 17 or at the 17/18 border (Horsley-Clarke coordinates 0–3 mm lateral and 5–9 mm posterior) with receptive fields within ~5° eccentricity. Results reported here concern 44 of the 71 cells for which we performed the drift rate experiment, and 30 of the 34 cells for which we performed the adaptation experiment. The cells included fulfilled the following requirements: (1) the maximum average response was greater than 5 spikes/s (15/71 and 0/34 cells excluded); (2) the ratio of the responses to test and mask was >1.5 (8/71 and 2/34 excluded); and(3) the model used to summarize the data accounted for >70% of the variance in the responses (4/71 and 1/34 excluded).

The descriptive model that we fitted to the responses is suited for both simple and complex cells. According to it, neurons receive a suppressive signal whose effect is to divide the responses by a measure of stimulus contrast. This suppressive signal is divisive and is provided by both test and mask.

The first stage of the model is linear in contrast: its responses to a sinusoidal grating are given by a constant B_i plus a sinusoid with amplitude A_i and phase P_i at the frequency ω_t of the stimulus, multiplied by stimulus contrast c_i:

$$L_i(t) = c_i[B_i + A_i \sin(2\pi\omega_t t + P_i)].$$

For a linear simple cell, B_i would be close to zero, whereas for a nonlinear complex cell, A_i would be close to zero (and thus P_i could be ignored).

The second stage of the model is nonlinear in contrast and incorporates a divisive suppressive signal. The output of the full model is given by

$$R(t) = \frac{\lfloor L_1(t) + L_2(t) - T \rfloor^n}{1 + (d_1 c_1)^n + (d_2 c_2)^n},$$

where c_1 and c_2 are test and mask contrast, L_1 and L_2 are the responses of the first stage to test and mask alone, the threshold T and the exponent n approximate the nonlinear effects of the encoding of membrane potential into firing rate, and d_1 and d_2 indicate the effectiveness of test and mask in suppressing the responses.

The simplified equation given in the Results section follows if a neuron (as is typical in V1) does not respond to the orthogonal orientation ($L_2 = 0$) and does not fire spontaneously ($T = 0$). Parameters of the reduced model were derived from those of the full model as follows. The suppression index k was taken to be the ratio d_2/d_1. The maximal response R_{max} was taken to be the response of the full model to a 100% contrast test in the absence of a mask. The half-maximal contrast c_{50} was taken to be the test contrast at which the response of the full model reached half of R_{max}.

We fitted the full model to the time-varying responses (Figure 1C), using a least-squares method. Fit quality was assessed by considering the percentage in the variance of a data set that was explained by the model. If m_j and r_j are the responses of the model and of the cell to the j-th stimulus, and r_0 is the mean of the responses, this percentage is

$$V = 100(1 - \Sigma_j(m_j - r_j)^2/\Sigma_j(r_j - r_0)^2).$$

The quality of the model fits was high. For data sets in the drift rate experiment (Figure 4), the model explained an average of 91.5% ± 5.3% (SD, n = 44) of the variance. For data sets in the adaptation experiment (Figure 5), the model explained an average of 89.2% ± 14.1% of the variance when adapting to the gray screen (n = 30), 89.8% ± 9.5% when adapting to the test (n = 28), and 91.4% ± 11.1% when adapting to the mask (n = 30). Data obtained in different adaptation conditions were fitted separately, but with a common value for the exponent n. Values of the exponent ranged from 1.8 to the highest value allowed, 5.0 (median: 2.32, n = 30). For the example V1 cell in Figure 1C, Figures 2A and 2B, Figure 5A, and Figures 6A and 6B, the fitting procedure yielded $n = 1.8$, and the model explained 98.9%, 96.5%, and 97.6% of the variance during adaptation to the gray screen, to the test, and to the mask. We can thus use the suppression index k to describe the effect of suppression in different adaptation conditions.

Data relating response to test drift rate (Figures 3A and 3C) and suppression index to mask drift rate (Figure 3E) were fitted with a descriptive function

$$y(x) = y_{max}\exp[-(x-x_{max})^2/\sigma(x)],$$

where $\sigma(x)$ is σ_- if $x < x_{max}$ and σ_+ if $x > x_{max}$, and y_{max}, x_{max}, σ_+ and σ_- are free parameters. This function yielded good fits. For example, for data relating V1 response to test drift rate (such as in Figure 3C), it explained >94% of the variance for half of the cells (n = 294), and <70% of the variance for only 11/294 cells. Estimates of suppression index (such as in Figure 3E) were noisier, and the descriptive function performed marginally worse: it explained >88% of the variance for half of the cells (n = 44), and <70% of the variance for 13/44 cells. Nonetheless, all fits appeared satisfactory, allowing us to obtain high-cut drift rates from fitted curves.

We recorded from 22 LGN neurons and performed the experiments in Figures 7A and 7C in 16 neurons, and the experiments in Figures 7B and 7D in 16 neurons. We found the responses of LGN neurons to be captured by a simple linear model, modified so that gain is affected by contrast (Shapley and Victor, 1981; 1978), and responses cannot be negative. The response of this model obeys the following expression:

$$R(t) = \lfloor R_{max}\frac{c_{test}\sin(\omega_{test}t + P_{test}) + rc_{mask}\sin(\omega_{mask}t + P_{mask})}{c_{50} + \sqrt{c_{test}^2 + (kc_{mask})^2}} - T\rfloor$$

Here, r determines the response to the mask relative to the response to the test, and k determines the ability of the mask to reduce the gain of the neuron, relative to that of the test.

Detailed methods for the synaptic depression model described in the Discussion are given elsewhere (M.C., D.J.H., and W.S., unpublished data). Here we concentrate on the basic features of the synaptic depression mechanism. We model depression at thalamocortical synapses by the following equation (Senn et al., 2001):

$$\frac{dp}{dt} = \frac{u - p}{\tau_R} - upf,$$

where p is the probability of synaptic transmission, f is the presynaptic firing rate, and u is the utilization parameter. Terms on the right-hand side govern recovery and depression. Depression (second term) is proportional to presynaptic firing rate f and to the utilization parameter u. An increase in f immediately reduces probability of synaptic transmission p. Recovery (first term) makes p return to the value u (if f is zero) over a time period determined by the time constant τ_R.

In our simulations, we set the utilization parameter to $u = 0.75$, at the high end of the range (0.1–0.95) found in vitro (Tsodyks and Markram, 1997). We set the time constant of recovery to $\tau_R = 200$ ms, intermediate between those reported for rapid depression in young animals (200–800 ms; Abbott et al., 1997; Varela et al., 1997) and in adult animals (60–70 ms, Thomson and Deuchars, 1997). Choosing different recovery time constants did not noticeably alter the results.

Acknowledgments

We are grateful to Valerio Mante and Vincent Bonin for help with the experiments, and to David Heeger and Walter Senn, who both collaborated with us on the synaptic depression model and provided crucial advice throughout the project. We also thank Massimo Scanziani for valuable discussions. This research was supported by Swiss National Science Foundation and by Human Frontiers Science Program Organization.

Received: December 27, 2001
Revised: June 3, 2002

References

Abbott, L.F., Varela, J.A., Sen, K., and Nelson, S.B. (1997). Synaptic depression and cortical gain control. Science *275*, 220–224.

Albrecht, D.G., and Geisler, W.S. (1991). Motion sensitivity and the contrast-response function of simple cells in the visual cortex. Vis. Neurosci. *7*, 531–546.

Albrecht, D.G., Farrar, S.B., and Hamilton, D.B. (1984). Spatial contrast adaptation characteristics of neurones recorded in the cat's visual cortex. J. Physiol. (Lond.) *347*, 713–739.

Allison, J.D., Smith, K.R., and Bonds, A.B. (2001). Temporal-frequency tuning of cross-orientation suppression in the cat striate cortex. Vis. Neurosci. *18*, 941–948.

Alonso, J.M., Usrey, W.M., and Reid, R.C. (2001). Rules of connectivity between geniculate cells and simple cells in cat primary visual cortex. J. Neurosci. *21*, 4002–4015.

Anderson, J., Carandini, M., and Ferster, D. (2000). Orientation tuning of input conductance, excitation and inhibition in cat primary visual cortex. J. Neurophysiol. *84*, 909–931.

Anderson, J.S., Lampl, I., Gillespie, D.C., and Ferster, D. (2001). Membrane potential and conductance changes underlying length tuning of cells in cat primary visual cortex. J. Neurosci. *21*, 2104–2112.

Bauman, L.A., and Bonds, A.B. (1991). Inhibitory refinement of spatial frequency selectivity in single cells of the cat striate cortex. Vision Res. *31*, 933–944.

Benevento, L.A., Creutzfeldt, O., and Kuhnt, U. (1972). Significance of intracortical inhibition in the visual cortex. Nature *238*, 124–126.

Blake, R. (2001). A primer on binocular rivalry, including current controversies. Brain & Mind *2*, 5–38.

Blakemore, C., and Tobin, E.A. (1972). Lateral inhibition between orientation detectors in the cat's visual cortex. Exp. Brain Res. *15*, 439–440.

Bolz, J., and Gilbert, C.D. (1986). Generation of end-inhibition in the visual cortex via interlaminar connections. Nature *320*, 362–365.

Bonds, A.B. (1989). Role of inhibition in the specification of orientation selectivity of cells in the cat striate cortex. Vis. Neurosci. *2*, 41–55.

Borg-Graham, L.J., Monier, C., and Frégnac, Y. (1998). Visual input evokes transient and strong shunting inhibition in visual cortical neurons. Nature *393*, 369–373.

Boynton, G.M., and Foley, J.M. (1999). Temporal sensitivity of human luminance pattern mechanisms determined by masking with temporally modulated stimuli. Vision Res. *39*, 1641–1656.

Brainard, D.H. (1997). The psychophysics toolbox. Spatial Vision *10*, 433–436.

Carandini, M., and Ferster, D. (1997). A tonic hyperpolarization underlying contrast adaptation in cat visual cortex. Science *276*, 949–952.

Carandini, M., and Ferster, D. (2000). Membrane potential and firing rate in cat primary visual cortex. J. Neurosci. *20*, 470–484.

Carandini, M., and Heeger, D.J. (1994). Summation and division by neurons in visual cortex. Science *264*, 1333–1336.

Carandini, M., Heeger, D.J., and Movshon, J.A. (1997). Linearity and normalization in simple cells of the macaque primary visual cortex. J. Neurosci. *17*, 8621–8644.

Carandini, M., Movshon, J.A., and Ferster, D. (1998). Pattern adaptation and cross-orientation interactions in the primary visual cortex. Neuropharmacology *37*, 501–511.

Chagnac-Amitai, Y., and Connors, B.W. (1989). Horizontal spread of synchronized activity in neocortex and its control by GABA-mediated inhibition. J. Neurophysiol. *61*, 747–758.

Chance, F.S., Nelson, S.B., and Abbott, L.F. (1998). Synaptic depression and the temporal response characteristics of V1 cells. J. Neurosci. *18*, 4785–4799.

Chung, S., Li, X., and Nelson, S.B. (2002). Short-term depression at thalamocortical synapses contributes to rapid adaptation of cortical sensory responses in vivo. Neuron *34*, 437–446.

Cohen, I., and Miles, R. (2000). Contributions of intrinsic and synaptic activities to the generation of neuronal discharges in in vitro hippocampus. J. Physiol. (Lond.) *524*, 485–502.

Crook, J.M., Kisvarday, Z.F., and Eysel, U.T. (1998). Evidence for a contribution of lateral inhibition to orientation tuning and direction selectivity in cat visual cortex: reversible inactivation of functionally characterized sites combined with neuroanatomical tracing techniques. Eur. J. Neurosci. *10*, 2056–2075.

DeAngelis, G.C., Robson, J.G., Ohzawa, I., and Freeman, R.D. (1992). The organization of supression in receptive fields of neurons in cat visual cortex. J. Neurophysiol. *68*, 144–163.

DeAngelis, G.C., Ohzawa, I., and Freeman, R.D. (1993). Spatiotemporal organization of simple-cell receptive fields in the cat's striate cortex. I. General characteristics and postnatal development. J. Neurophysiol. *69*, 1091–1117.

DeAngelis, G.C., Freeman, R.D., and Ohzawa, I. (1994). Length and width tuning of neurons in the cat's primary visual cortex. J. Neurophysiol. *71*, 347–374.

Douglas, R.J., Martin, K.A.C., and Whitteridge, D. (1988). Selective responses of visual cortical cells do not depend on shunting inhibition. Nature *332*, 642–644.

Eysel, U.T., Crook, J.M., and Machemer, H.F. (1990). GABA-induced remote inactivation reveal cross-orientation inhibition in the cat striate cortex. Exp. Brain Res. *80*, 626–630.

Ferster, D. (1988). Spatially opponent excitation and inhibition in simple cells of the cat visual cortex. J. Neurosci. *8*, 1172–1180.

Ferster, D., and Lindström, S. (1985). Augmenting responses evoked in area 17 of the cat by intracortical axons collaterals of corticogeniculate cells. J. Physiol. (Lond.) *367*, 217–232.

Ferster, D., and Miller, K.D. (2000). Neural mechanisms of orientation selectivity in the visual cortex. Annu. Rev. Neurosci. *23*, 441–471.

Fitzpatrick, D. (2000). Seeing beyond the receptive field in primary visual cortex. Curr. Opin. Neurobiol. *10*, 438–443.

Foley, J.M., and Chen, C.C. (1997). Analysis of the effect of pattern adaptation on pattern pedestal effects: a two-process model. Vision Res. *37*, 2779–2788.

Gilbert, C.D., and Kelly, J.P. (1975). The projections of cells in different layers of the cat's visual cortex. J. Comp. Neurol. *163*, 81–106.

Glezer, V.D., Tscherbach, T.A., Gauselman, V.E., and Bondarko, V.E. (1982). Spatio-temporal organization of receptive fields of the cat striate cortex. Biol. Cybern. *43*, 35–49.

Grieve, K.L., and Sillito, A.M. (1991). A re-appraisal of the role of layer VI of the visual cortex in the generation of cortical end inhibition. Exp. Brain Res. *87*, 521–529.

Heeger, D.J. (1992). Normalization of cell responses in cat striate cortex. Vis. Neurosci. *9*, 181–197.

Hirsch, J.A., Alonso, J.M., Reid, R.C., and Martinez, L.M. (1998). Synaptic integration in striate cortical simple cells. J. Neurosci. *18*, 9517–9528.

Hubel, D., and Wiesel, T. (1965). Receptive fields and functional architecture in two nonstriate visual areas (18-19) of the cat. J. Neurophysiol. *28*, 229–289.

Hubel, D.H., and Wiesel, T.N. (1962). Receptive fields, binocular interaction and functional architecture in the cat's visual cortex. J. Physiol. (Lond.) *160*, 106–154.

Ikeda, H., and Wright, M.J. (1975). Spatial and temporal properties of 'sustained' and 'transient' neurones in area 17 of the cat's visual cortex. Exp. Brain Res. *22*, 363–383.

Kayser, A., Priebe, N.J., and Miller, K.D. (2001). Contrast-dependent nonlinearities arise locally in a model of contrast- invariant orientation tuning. J. Neurophysiol. *85*, 2130–2149.

Koch, C., Poggio, T., and Torre, V. (1983). Nonlinear interactions in a dendritic tree: localization, timing, and role in information processing. Proc. Natl. Acad. Sci. USA *80*, 2799–2802.

Lauritzen, T.Z., Krukowski, A.E., and Miller, K.D. (2001). Local correlation-based circuitry can account for responses to multi-grating stimuli in a model of cat V1. J. Neurophysiol. *86*, 1803–1815.

Li, C.-Y., and Li, W. (1994). Extensive integration beyond the classical receptive field of cat's striate cortical neurons–classification and tuning properties. Vision Res. *34*, 2337–2356.

Maffei, L., Fiorentini, A., and Bisti, S. (1973). Neural correlate of perceptual adaptation to gratings. Science *182*, 1036–1038.

Martinez, L.M., Alonso, J.M., Reid, R.C., and Hirsch, J.A. (2002). Laminar processing of stimulus orientation in cat visual cortex. J. Physiol. (Lond.) *540*, 321–333.

McCormick, D.A., Connors, B.W., Lighthall, J.W., and Prince, D.A. (1985). Comparative electrophysiology of pyramidal and sparsely spiny stellate neurons of the neocortex. J. Neurophysiol. *54*, 782–806.

Meier, L., and Carandini, M. (2002). Masking with fast gratings. Journal of Vision. Published online July 12, 2002. 10.1167/2.4.2.

Morrone, M.C., Burr, D.C., and Maffei, L. (1982). Functional implications of cross-orientation inhibition of cortical visual cells. I. Neurophysiological evidence. Proc. R. Soc. Lond. B Biol. Sci. *216*, 335–354.

Morrone, M.C., Burr, D.C., and Speed, H.D. (1987). Cross-orientation inhibition in cat is GABA mediated. Exp. Brain Res. *67*, 635–644.

Movshon, J.A., and Lennie, P. (1979). Pattern-selective adaptation in visual cortical neurones. Nature *278*, 850–852.

Movshon, J.A., Thompson, I.D., and Tolhurst, D.J. (1978). Spatial and temporal contrast sensitivity of neurones in areas 17 and 18 of the cat's visual cortex. J. Physiol. (Lond.) *283*, 101–120.

Müller, J.R., Metha, A.B., Krauskopf, J., and Lennie, P. (1999). Rapid adaptation in visual cortex to the structure of images. Science *285*, 1405–1408.

Müller, J.R., Metha, A.B., Krauskopf, J., and Lennie, P. (2001). Information conveyed by onset transients in responses of striate cortical neurons. J. Neurosci. *21*, 6978–6990.

Murphy, P.C., and Sillito, A.M. (1987). Corticofugal feedback influences the generation of length tuning in the visual pathway. Nature *329*, 727–729.

Murphy, P.C., Duckett, S.G., and Sillito, A.M. (1999). Feedback connections to the lateral geniculate nucleus and cortical response properties. Science *286*, 1552–1554.

Nelson, S.B. (1991a). Temporal interactions in the cat visual system I. Orientation-selective suppression in visual cortex. J. Neurosci. *11*, 344–356.

Nelson, S.B. (1991b). Temporal interactions in the cat visual system II. Facilitatory effects in the lateral geniculate nucleus. J. Neurosci. *11*, 357–368.

Nelson, S.B. (1991c). Temporal interactions in the cat visual system III. Pharmacological studies of cortical suppression suggest a presynaptic mechanism. J. Neurosci. *11*, 369–380.

Nelson, S., Toth, L., Sheth, B., and Sur, M. (1994). Orientation selectivity of cortical neurons during intracellular blockade of inhibition. Science *265*, 774–777.

Ohzawa, I., Sclar, G., and Freeman, R.D. (1985). Contrast gain control in the cat visual system. J. Neurophysiol. *54*, 651–665.

Palmer, L.A., and Davis, T.L. (1981). Receptive-field structure in cat striate cortex. J. Neurophysiol. *46*, 260–276.

Payne, B.R., and Peters, A. (2002). The concept of cat primary visual cortex. In The Cat Primary Visual Cortex, B.R. Payne and A. Peters, eds. (New York: Academic Press), pp. 1–137.

Pelli, D.G. (1997). The VideoToolbox software for visual psychophysics: transforming numbers into movies. Spat. Vis. *10*, 437–442.

Reid, R.C., and Alonso, J.M. (1995). Specificity of monosynaptic connections from thalamus to visual cortex. Nature *378*, 281–284.

Reid, R.C., Victor, J.D., and Shapley, R.M. (1992). Broadband temporal stimuli decrease the integration time of neuron in cat striate cortex. Vis. Neurosci. *9*, 39–45.

Robinson, D.A. (1968). The electrical properties of metal microelectrodes. Proceedings of the IEEE *56*, 1065–1071.

Sanchez-Vives, M.V., Nowak, L.G., and McCormick, D.A. (2000). Membrane mechanisms underlying contrast adaptation in cat area 17 in vivo. J. Neurosci. *20*, 4267–4285.

Saul, A.B., and Humphrey, A.L. (1990). Spatial and temporal response properties of lagged and nonlagged cells in cat lateral geniculate nucleus. J. Neurophysiol. *64*, 206–224.

Saul, A.B., and Humphrey, A.L. (1992). Temporal-frequency tuning of direction selectivity in cat visual cortex. Vis. Neurosci. *8*, 365–372.

Schwartz, O., and Simoncelli, E.P. (2001). Natural signal statistics and sensory gain control. Nat. Neurosci. *4*, 819–825.

Sclar, G., Maunsell, J.H.R., and Lennie, P. (1990). Coding of image

contrast in central visual pathways of the macaque monkey. Vision Res. *30*, 1–10.

Sengpiel, F., and Blakemore, C. (1994). Interocular control of neuronal responsiveness in cat visual cortex. Nature *368*, 847–850.

Sengpiel, F., Blakemore, C., and Harrad, R. (1995). Interocular suppression in the primary visual cortex: a possible neural basis of binocular rivalry. Vision Res. *35*, 179–196.

Sengpiel, F., Baddeley, R.J., Freeman, T.C., Harrad, R., and Blakemore, C. (1998). Different mechanisms underlie three inhibitory phenomena in cat area 17. Vision Res. *38*, 2067–2080.

Senn, W., Markram, H., and Tsodyks, M. (2001). An algorithm for modifying neurotransmitter release probability based on pre- and postsynaptic spike timing. Neural Comput. *13*, 35–67.

Shapley, R.M., and Victor, J. (1981). How the contrast gain modifies the frequency responses of cat retinal ganglion cells. J. Physiol. (Lond.) *318*, 161–179.

Shapley, R.M., and Victor, J.D. (1978). The effect of contrast on the transfer properties of cat retinal ganglion cells. J. Physiol. (Lond.) *285*, 275–298.

Shou, T., Li, X., Zhou, Y., and Hu, B. (1996). Adaptation of visually evoked responses of relay cells in the dorsal lateral geniculate nucleus of the cat following prolonged exposure to drifting gratings. Vis. Neurosci. *13*, 605–613.

Sillito, A.M. (1975). The contribution of inhibitory mechanisms to the receptive field properties of neurones in the cat's striate cortex. J. Physiol. (Lond.) *250*, 304–330.

Smith, M.A., Bair, W., Cavanaugh, J.R., and Movshon, J.A. (2001). Latency of inhibition from inside and outside the classical receptive field in macaque V1 neurons. Journal of Vision. Published online December 12, 2001. 10.1167/1.3.35.

Sompolinsky, H., and Shapley, R. (1997). New perspectives on the mechanisms for orientation selectivity. Curr. Opin. Neurobiol. *7*, 514–522.

Stratford, K.J., Tarczy-Hornoch, K., Martin, K.A.C., Bannister, N.J., and Jack, J.J. (1996). Excitatory synaptic inputs to spiny stellate cells in cat visual cortex. Nature *382*, 258–261.

Thomson, A.M., and Deuchars, J. (1997). Synaptic interactions in neocortical local circuits: dual intracellular recordings in vitro. Cereb. Cortex *7*, 510–522.

Tolhurst, D.J., and Dean, A.F. (1987). Spatial summation by simple cells in the striate cortex of the cat. Exp. Brain Res. *66*, 607–620.

Tolhurst, D.J., and Dean, A.F. (1990). The effects of contrast on the linearity of spatial summation of simple cell in the cat's striate cortex. Exp. Brain Res. *79*, 582–588.

Tolhurst, D.J., Walker, N.S., Thompson, I.D., and Dean, A.F. (1980). Nonlinearities of temporal summation in neurones in area 17 of the cat. Exp. Brain Res. *38*, 431–435.

Troyer, T.W., Krukowski, A.E., Priebe, N.J., and Miller, K.D. (1998). Contrast-invariant orientation tuning in cat visual cortex: thalamocortical input tuning and correlation-based intracortical connectivity. J. Neurosci. *18*, 5908–5927.

Tsodyks, M.V., and Markram, H. (1997). The neural code between neocortical pyramidal neurons depends on neurotransmitter release probability. Proc. Natl. Acad. Sci. USA *94*, 719–723.

Varela, J.A., Sen, K., Gibson, J., Fost, J., Abbott, L.F., and Nelson, S.B. (1997). A quantitative description of short-term plasticity at excitatory synapses in layer 2/3 of rat primary visual cortex. J. Neurosci. *17*, 7926–7940.

Vidyasagar, T.R., Pei, X., and Volgushev, M. (1996). Multiple mechanisms underlying the orientation selectivity of visual cortical neurones. Trends Neurosci. *19*, 272–277.

Walker, G.A., Ohzawa, I., and Freeman, R.D. (1998). Binocular cross-orientation suppression in the cat's striate cortex. J. Neurophysiol. *79*, 227–239.